Russell-Pavier, F., Picco, L., Payton, O., Day, J., Shatil, N., & Yacoot, A. (2018). 'Hi-Fi AFM': high-speed contact mode atomic force microscopy with optical pickups. *Measurement Science and Technology*. https://doi.org/10.1088/1361-6501/aad771

‘Hi-Fi AFM’: high-speed contact mode atomic force microscopy with optical pickups

F S Russell-Pavier[1,3], L Picco[1,4], J C C Day[1], N Shatil[2], A Yacoot[3] and O D Payton[1,2,4]

1. Interface Analysis Centre, H. H. Wills Laboratory, University of Bristol, BS8 1TL
2. Engineering Maths, Merchant Ventures Building, University of Bristol, BS8 1UB
3. The National Physical Laboratory, Hampton Road, Teddington, Middlesex, TW11 0LW
4. Bristol Nano Dynamics, Bristol, BS1 6HL

Author email: freddie.russell-pavier@bristol.ac.uk

Abstract. High-speed atomic force microscopy (HS-AFM) is a powerful emerging technique used to gain insight into real-time nanoscale dynamics and phenomena across the sciences. By performing measurements of material properties, abundancy counting and dimensional analysis, it enables a new generation of discoveries at the atomic scale. Here, we demonstrate the use of an optical pickup unit (OPU) typically found in PCs, Hi-Fis and games consoles worldwide, as a vertical detection system within in a HS-AFM operated in contact mode. The OPU displacement performance is compared to that of a commercially available laser Doppler vibrometer with ±15 pm resolution. Sub-nanometre sensitivity is achieved with an OPU, presented via the identification of two resonant modes of a cantilever stimulated by ambient thermal excitation. To demonstrate the large dynamic range of the sensor at fast scan-speeds, surface profiles with step heights in excess of 100 nm and surface textures less than 10 nm were collected using a custom OPU based HS-AFM. The high fidelity measurements are extended to visible length scales in short timescales by imaging areas of up to 200 µm^2 area at a pixel rate of 2 megapixels/s, tip velocity of 10 mm/s and area rate of 25 µm^2/s.

PACS: 07.79.-v, 42.15.Eq, 81.07.-b

Submitted to: Measurement Science and Technology, Institute of Physics

1. Background

Optical pickup units (OPUs), developed for reading or writing to optical discs such as CD, DVD and Blu-Ray, have already shown potential as low-cost nanoscale sensors within a number of applications. These include AFMs, straightness measurement devices and touch trigger probes, amongst others[1–7]. Building upon the mass-production of these devices proves an effective way to develop new measurement capabilities.

OPUs are designed with several optical and mechanical properties that are advantageous for use as high-bandwidth nanoscale displacement sensors. Firstly, the outgoing laser beam is focussed through an objective lens to a sub-micron sized spot. Additionally, the OPU contains an inbuilt quadrant photodiode with an operational bandwidth of tens to hundreds of MHz, and the ability to translate internal optical components with nanometre resolution[8]. Coincidentally, the OPU’s capabilities are ideally suited for the monitoring of micro-mechanical cantilevers used in atomic force microscopy (AFM) for surface profile measurements. The change of application space for OPUs in this way was first demonstrated by Quercioli *et al.* with a CD OPU in 1999[2]. Since then, studies have demonstrated the use of OPUs within traditional forms of AFM. These methods are constrained by physical and electrical properties, as described later, which do not permit for the full utilization of the higher bandwidths that the OPUs are capable of sensing. Importantly, OPUs also promise a large increase in measurement scope and throughput, by facilitating simultaneous 2D angular and displacement measurements[9].

1.1. High-speed atomic force microscopy (HS-AFM)

Historically, AFM has been known to produce topographical maps at a rate of line scans per second, or frames per hour. Consequently, it has been considered by many as too slow to be a viable method to practically characterize large sample areas (square millimetres). Since the inception of AFM[10], surface probe techniques have been developed in a variety of imaging modes[11–13], and varied according to the sample and measurement requirements. One variant which improves upon rates of previously demonstrated techniques is HS-AFM[14–16].

Significant breakthroughs by Payton *et al.* showed that by measuring the displacement of the known node above the tip on the cantilever, rather than taking an angular measurement via beam deflection[17], the resultant height map would be less susceptible to unwanted flexural and torsional vibrational modes excited along the cantilever[18]. This is an important consideration when imaging at higher-speeds, as higher-tip velocities over the surface allow for greater excitation of the cantilever’s resonant modes. Furthermore, by using a cantilever with a low spring constant and high compliance to the surface topography, the system can be operated without an active constant height mode control loop. This reduces the digital processing time required for each height measurement compared with other implementations [19–22] and enables scanning at high-rates.

Statistical confidence in measured sample properties is enhanced by HS-AFM, since it can be used to collect many frames in short time periods (minutes) with high pixel density. Generating the equivalent number of frames with the same resolution, at the more typical lower rates common to traditional AFMs (hours-days), is impractical and can lead to less populous datasets being collected over a smaller imaging areas. This in turn can result in assumptions of homogeneity across the sample being inferred from a relatively small measured sample size. Crucially, this may translate to selective bias in the measurement of material properties. A key benefit of HS-AFM is that it takes much less time to analyse the material properties of the sample surface, which allows measurements to be taken over longer distance and larger areas, enabling nanoscale measurements to be linked to microscopic length scales. In other applications, the temporal resolution allows dynamic behaviour at the nanoscale to be observed[23–26].

The existing commercial HS-AFM used in this work, incorporating a laser Doppler-shift vibrometer (LDV) to detect the cantilever’s motion, has been developed by Bristol Nano Dynamics Ltd. and the University of Bristol. The LDV detection system (OFV-534) and decoder card (DD-900) made by Polytec GmbH, can collect 2.5 million measurements of the cantilever displacement per second, with a resolution of ±15 pm. This enables the HS-AFM to resolve atomic steps with multiple frames per second. This HS-AFM has been shown to be an extremely useful tool when conducting analyses of 2D materials[27,28] and genomic mapping[29]. In both cases, the increased speed has permitted the measurement of nanometre and sub-nanometre features at tens to hundreds of times per minute. This allows for large sample sizes to be measured in practical timeframes.

1.2. Typical optical pickup unit (OPU) functionality

An OPU maintains laser focus on the optical media disc using an optical astigmatic detection system (ADS). Within the ADS, a quadrant photodiode (QPD) is used to read encoded digital information on the disc. This is done by detecting whether the laser spot is incident on a high (land) or low (pit) area of the optical track. The QPD also generates a measure of the focus error (FE) of the laser relative to the disc surface. The FE measurement is taken by focusing the returning astigmatic laser beam onto the QPD. When focussed through a lens, the astigmatic beam has two orthogonal focal planes: the sagittal and tangential. These focal planes are offset in space by a fixed distance that is a property of the emission laser. The laser is deemed in-focus when the reflected beam falls symmetrically about the centre point of the two focal planes. If true, each quadrant in the QPD contributes equally to the FE signal (figure 1(b)). At the focal range limit the beam is predominantly focussed onto one of the two focal planes (figure 1(a) or (c)). The focus error signal (FES) is calculated using equation 1 from the QPD signals, as labelled in figure 1.

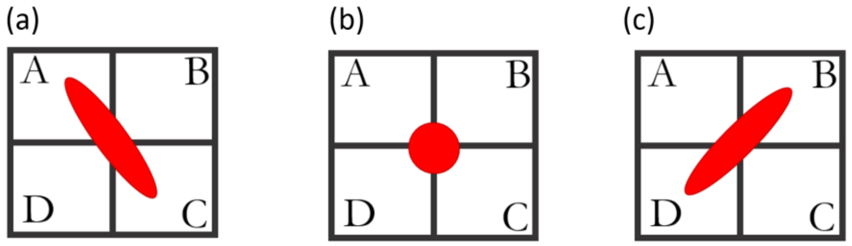

Figure 1. A QPD with the quadrants labelled (A-D). The three most distinct focal regimes of the astigmatic detection system are shown ((a)-(c)). The beam profile incident on the QPD is shown in each case.

$$\widehat{FES} = \frac{(\mathrm{A}+\mathrm{C})-(\mathrm{B}+\mathrm{D})}{A+B+C+D} \qquad (1)$$

In this work we use a Sanyo SF-HD65 OPU as shown in figure 2. This model has been integrated into a variety of CD/DVD-ROM drives for more than a decade. The focal length of the objective lens is 3.05 mm and the numerical aperture is 0.60 for the DVD laser (650 nm). An aberration correction plate similar to the substrate found on the underside of a DVD can be placed between objective lens (5) and the cantilever (6) (see figure 2(b)) and used to vary the desired ADS sensitivity. A key benefit of this model is the use of an on-board high-frequency module (HFM) with a single-mode dual laser diode which in combination act to minimise the required laser drive current and relative intensity noise.

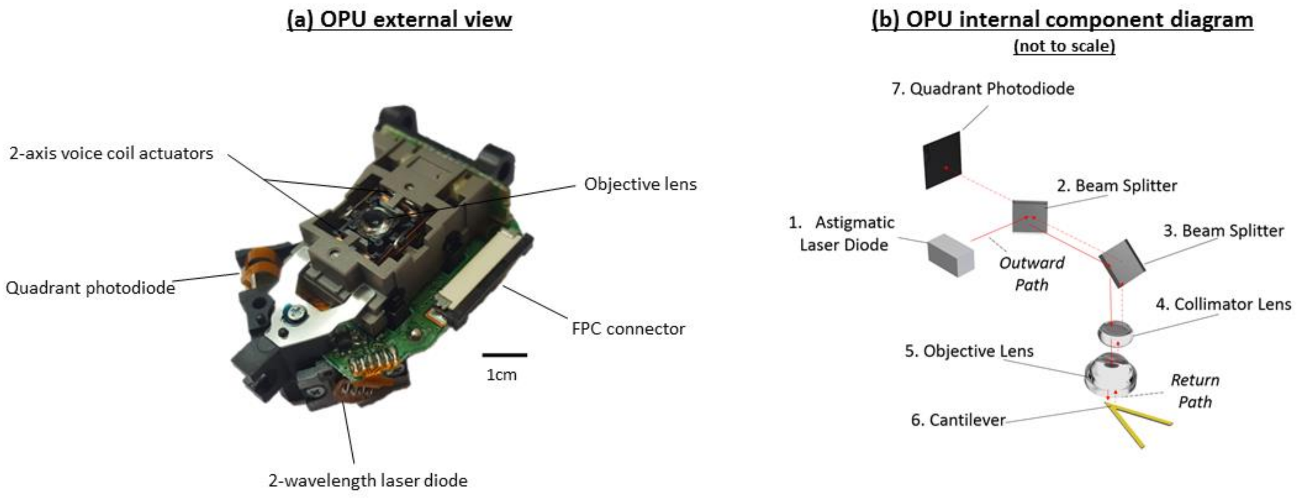

Figure 2. (a) An external photo of the Sanyo-HD65 OPU with visible components labelled with scale bar and (b) a labelled internal component diagram.

For each of the optical media disc pickup types (CD/DVD/Blu-Ray) a different typical operational inter-focal plane distance is used. These are typically 9 µm (CD), 6 µm (DVD) and 3 µm (Blu-Ray)[30]. The FES from the DVD laser on board the Sanyo SF-HD65 is plotted as a function of displacement, seen in figure 3. This was determined by placing a reflective silicon (Si) wafer on a calibrated nano-positioning stage (NPXY60Z20-257, nPoint US). The displacement of the wafer was measured by digitising the inbuilt capacitance sensors in the stage using a National Instruments (USB-6363) data acquisition (DAQ) box. This DAQ simultaneously measured the QPD output which was used to calculate the FES signal.

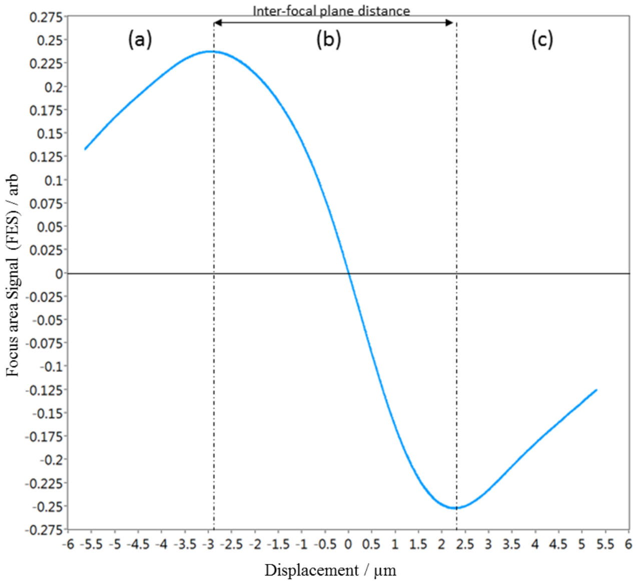

Figure 3: The focus error signal against linear displacement, typically known as the 'S-curve', with three distinct focal regimes labelled (a), (b) and (c).

Previous instrumentation research with OPUs have been seen in a large number of exciting configurations for bio-sensing and material analysis[7,31–33]. Studies of OPUs as a detection system in AFMs have primarily focussed on tapping mode and at lower rates than reported here[2,8,9,34–36]. A study of HS-AFM demonstrated in tapping mode, with a specially manufactured small cantilever with resonant frequency >1 MHz, has been reported[6]. This was used to image at rates up to 1.4 mm/s. Higher speeds were made possible by reducing the cantilever to dimensions much below those found in typical cantilevers, but this increase in speed is limited by the achievable, practical reduction in dimensions. Whilst a contact mode configuration has previously been reported[35,37], the method differs from that explored here. The methodology from the work presented here promises full utilisation of the OPU bandwidth (tens to hundreds of MHz), which gives tremendous potential for HS-AFM to spatially map materials, across nine orders of magnitude, within hours.

This work further evaluates an imaging mode and instrumentation that was summarised in an application focussed paper on DNA nanomapping [29] for genomic research. Further details of its implementation, evaluation, measurement properties and extensions to larger image area are reported here. A side by side comparison an OPU based HS-AFM is compared with a commercial HS-AFM for video rate AFM. In addition, measurements of the dynamics of a free cantilever are compared with theory and the commercial HS-AFM to establish a noise floor and minimum displacement sensitivity for the OPU detection head across the operational frequency range used for HS-AFM.

2. Method

2.1. Incorporating an OPU into the HS-AFM

For contact mode HS-AFM the OPU can be incorporated as a detection system, as illustrated in figure 4. A flexible contact mode cantilever (MSNL-C, Bruker) with a spring constant of 0.01 N/m is used. Figure 4 also shows how the cantilever, sample and high-speed parallel flexure stage are positioned in relation to one another.

Here, a purpose-built dual axis parallel flexure stage, spark eroded from an aluminium block, is used as the HS-AFM scan stage. Ceramic piezoelectric actuators (SA050510, PiezoDrive) on each axis are used to generate a high-aspect ratio (1:1000 Hz) Lissajous path. These actuators enable the sample to be scanned underneath the cantilever at rates of up to 64 µm^2/second. The mechanical performance of the flexure stage and the Lissajous path parameters allows each fundamental cantilever measurement to be used inter-changeably for increased frame rate or frame area. Such that either large areas (e.g. 1-64 µm^2) can be imaged at 1 Hz, or smaller areas (e.g. < 1 µm^2) at tens of Hz. The number of pixels in each frame is variable depending on the chosen frame rate. However, regardless of frame rate a total number of 2 megapixels, with 16-bit depth, are collected per second by this instrument.

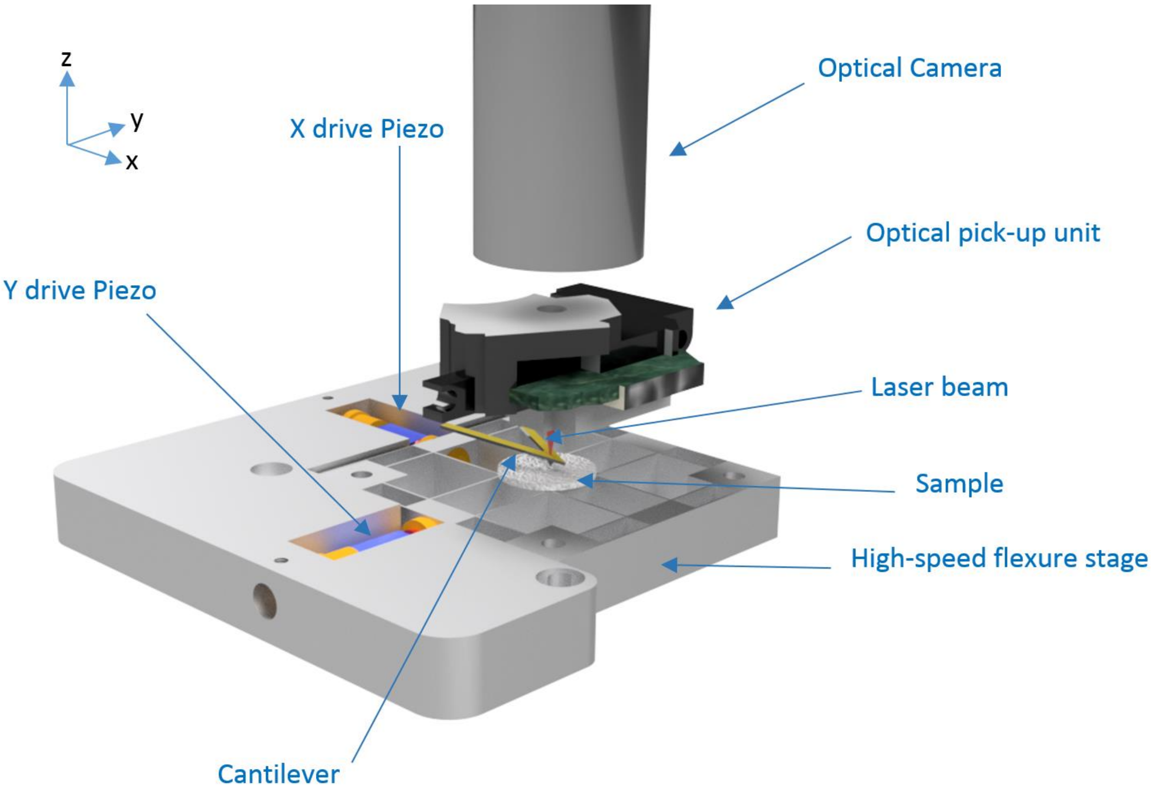

Figure 4: A simplified 3D schematic of an OPU based HS-AFM, with key components labelled (not to scale).

As OPUs aren’t typically used in the configuration described in figure 4, custom electronics have to be produced to provide automatic power control to the laser, and to allow for position control of the objective lens. The principle aim of the system is to position the laser spot accurately and stably on the cantilever, to translate the sample underneath the cantilever and to acquire the FES from the QPD. An overview, summarized with a system diagram, can be found in figure 5.

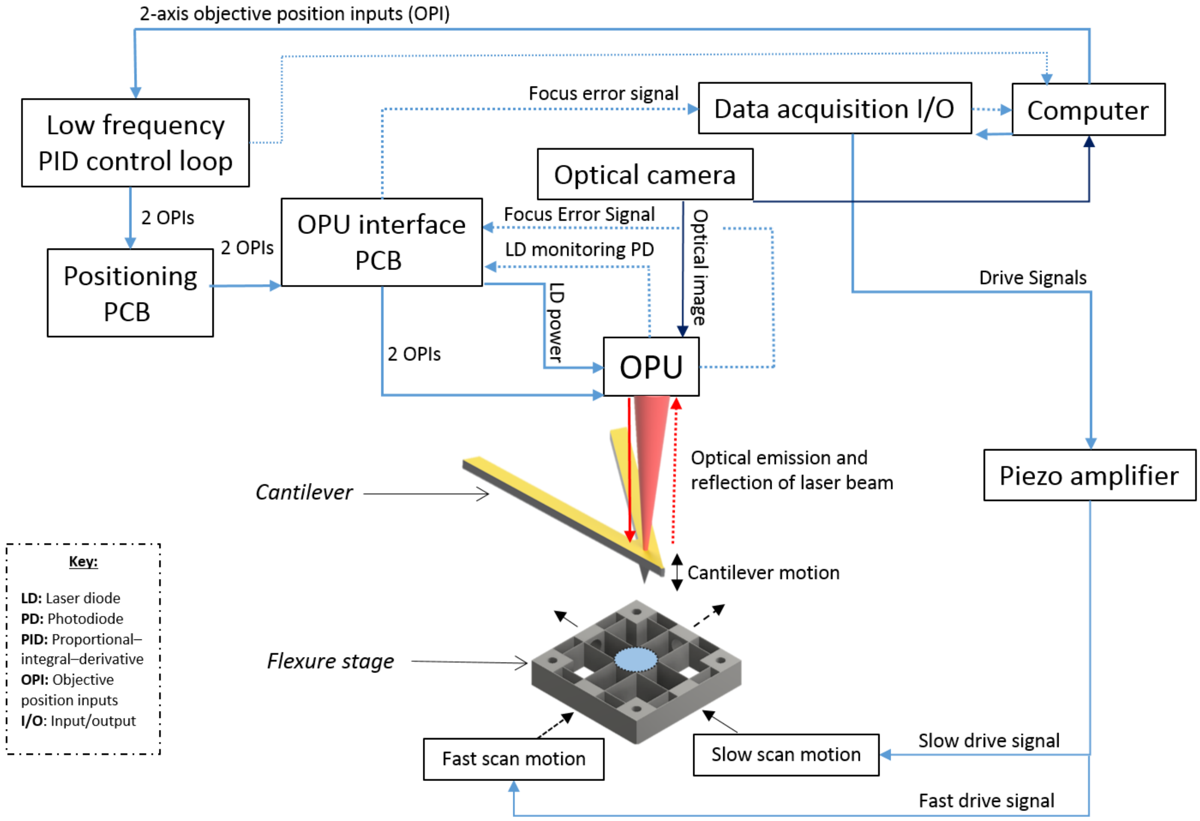

Figure 5: System schematic of an OPU based HS-AFM to computer interface, with key components labelled.

3 Results

3.1. Displacement sensing of the cantilever

The optical image, shown in figure 6, demonstrates that the OPU can be used as an optical microscope by utilising the optical path through the objective lens. The objective lens is translated and focussed by the inbuilt voice coil actuators. The microscope can be used for identifying the position of the laser spot and the cantilever. It is also essential for ensuring that the laser spot is correctly placed directly above the tip of the cantilever. The optical image can also focus on the sample, allowing regions of interest to be found prior to engaging the cantilever into contact with the surface.

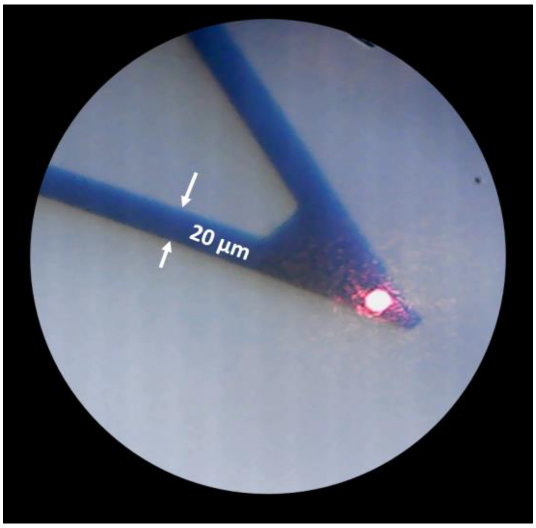

Figure 6. The optical view through Sanyo HD65 OPU of laser spot incident on an MSNL – C cantilever.

To test the fidelity and alignment of the detection system, the FE displacement measurement can be used to identify the resonant modes of the free cantilever due to thermal excitations in air and calculate the sensitivity of the ADS. We use the model outlined by Stark *et al.*[38] to predict the resonant frequency amplitudes of these expected thermomechanical contributions to the signal as shown in figure 7.

Using this model for the thermal excitation of the MSNL-C cantilever, the amplitudes of the first two modes are expected to be 0.838 nm ± 0.24 nm and 0.125 nm ± 0.04 nm. Here, we assume the parallel beam approximation (PBA) to compensate for the v-shaped geometry of the cantilever. In addition, we assume that thermal energy is only imparted from the surrounding thermal bath and that there is no significant thermal excitation from the laser (typically 0.3 mW at OPU output). It is then possible to identify these experimentally by looking at the power spectral density of the focus error signal whilst the laser incident on the MSNL-C cantilever:

$$S_p(f) = \frac{\Delta t}{T} \left| \sum_{n=1}^{N} v_n e^{-ifn} \right|^2 . \qquad (2)$$

Where the power spectral density, (S_p), is a function of the frequency components, (f), in the signal made up of discrete voltages, (v_n), sampled in Δt over a time period, (T), in 1 second. By taking a power spectrum, sampled at 2 MHz, for both the OPU and LDV signal responses it is possible to identify the first two resonant modes and measure their contributions to the signal.

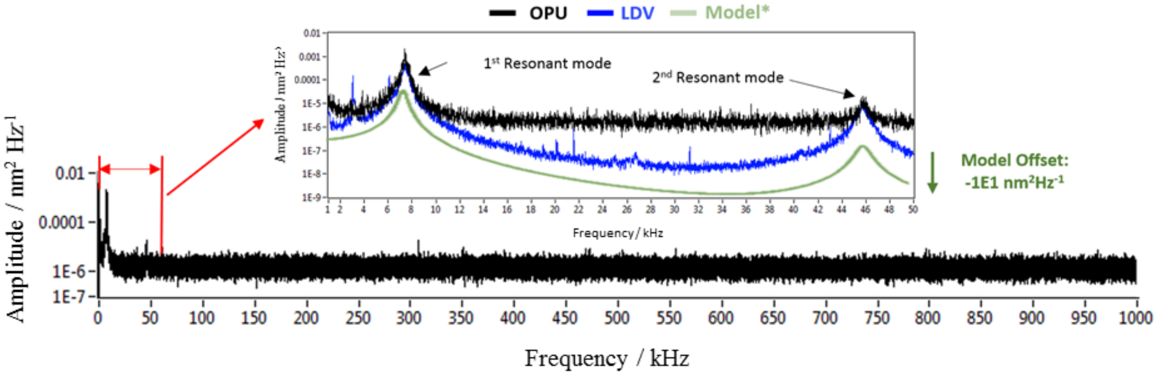

Figure 7: The power spectral density (PSD) of the OPU’s focus error signal (black) for a cantilever in free air. The 1st and 2nd modes can be seen at the expected locations in the sub-section of a spectrum and plotted with the LDV PSD (blue). The model (green) is offset in plot for comparison against data.

By looking in the frequency domain, resonances excited by the thermal energy in the room at (293.2 K) were identified. The first peak was found at 7.44 kHz ± 0.24 kHz. This corresponds to the first flexural resonant frequency expected for the MSNL-C cantilever specified as 7 kHz ± 3 kHz by the manufacturers. The amplitude for this mode was found to be 0.631 nm ± 0.11 nm. The second peak was found at 45.8 kHz ± 0.35 kHz with an amplitude 0.117 nm ± 0.05 nm corresponding to the 2nd predicted resonant mode. In both cases, there is a slight overestimation of the amplitudes but they are within error margins so otherwise there is good agreement to the model. The noise floor across the entire spectrum of the PSD is flat and approximately equal to 5 $\mathrm{pm}^2\,\mathrm{kHz}^{-1}$.

3.2. HS-AFM imaging comparison

To compare the imaging capabilities of the OPU and the LDV HS-AFM a grid of square pits arranged it a ‘waffle’ pattern, formed from titanium evaporated onto a flat silicon substrate, was measured (figure 8). In each case the sample was mounted on the same scanner and imaged with a scan amplitude 5 µm × 5 µm. Each HS-AFM image has 0.5 megapixels (500 by 1000 pixels) and took 0.5 seconds to collect, with no flattening or other correction of the image used. Compared with traditional AFM imaging speed metrics this is equivalent to a rate of 2000 lines per second. In a given second four images are produced of 500 x 1000 pixels. As common in scanning probe microscopy the images are split dependent on the direction of motion of the high-aspect Lissajous path: trace (t) or retrace (r) in either the fast (F) or slow (S) scan. Giving the following combinations that classify four images, generated per second, in a given pass of the high-aspect Lissajous path: F_t, F_r, S_t and S_r.

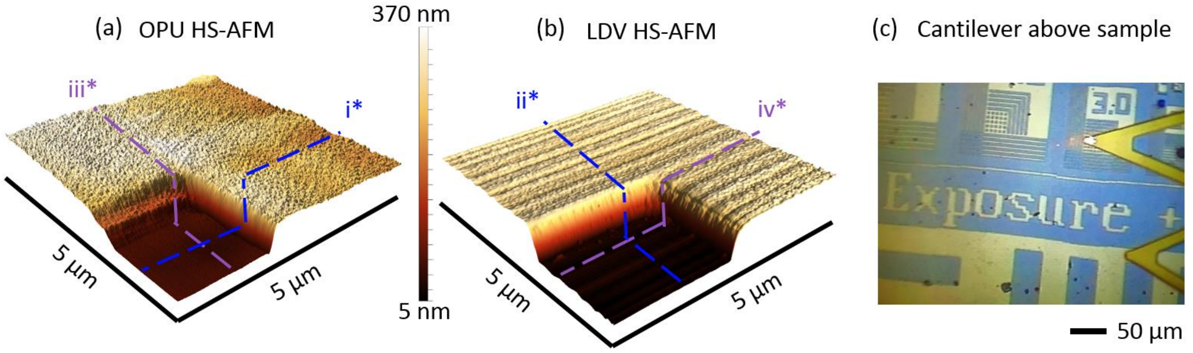

Figure 8: A presentation of unfiltered data from the sample (a) A 5 µm by 5 µm map of the silicon-titanium grid made using the OPU based HS-AFM. (b) A 5 µm by 5 µm map of a silicon-titanium grid made using the LDV based HS-AFM. (c) An optical image, taken on the commercial system, with the location of HS-AFM image on sample labelled

By looking at the line profiles (figure 9) across the two surfaces it is possible to see the contrast in the heights of the two materials. Furthermore, for the OPU line scan, the contrast in the height deviation or roughness from the higher regions is much more than that in the lower regions, as expected due to the contrast in surface texture between silicon wafer and evaporated titanium.

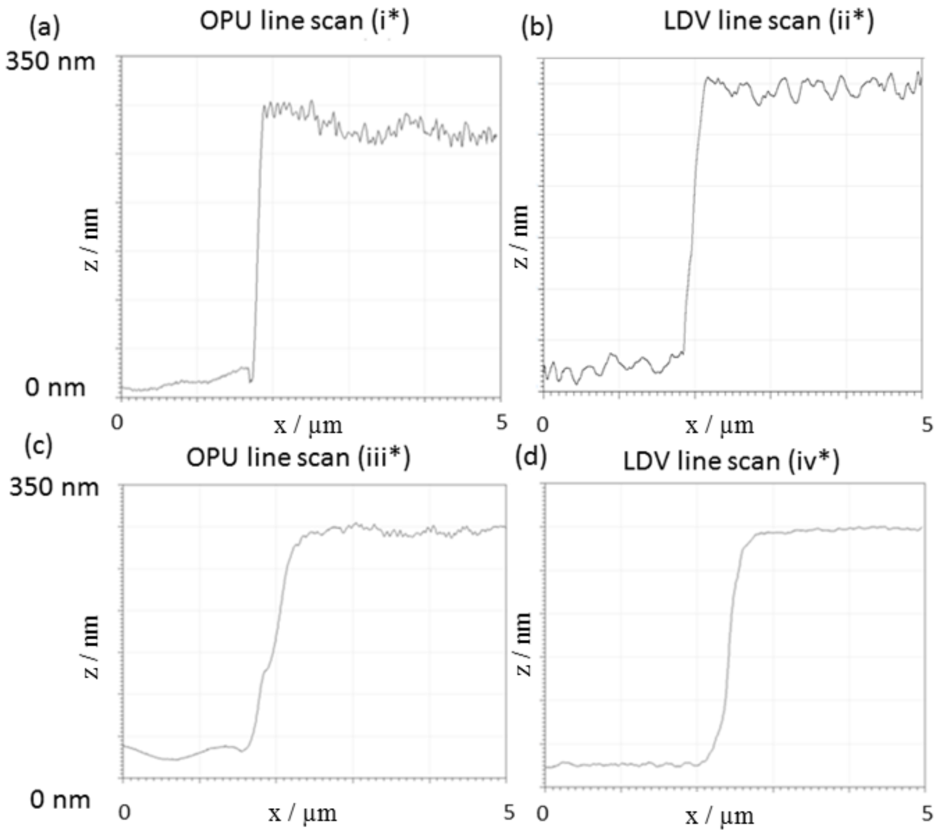

Figure 9. (a)-(d) Line scans showing the cross-section through the OPU and LDV based HS-AFM datasets labelled by the lines (i*-iv*) in figure 9.

Figure 9 demonstrates the technique's ability to successfully image step heights greater than 250 nm, while still tracking the surface roughness of the material with enough resolution to distinguish between the two materials.

By taking a profile from the lower and upper regions of the surfaces (Supplementary Table 1), it is possible to calculate the RMS roughness (Rq) for each, as measured by the two systems. For the lower region Rq was found to be 0.4 nm (OPU) and 0.3 nm (LDV). For the higher regions Rq was found to be 1.9 nm (OPU) and 1.6 nm (LDV). The distinct values allow the classification of the two materials. The discrepancy in Rq between the two systems is mainly due to a variance in tip radius, noise floor contributions (figure 7) and post-process flattening. The manufacturers specify the tip radius can range from 2-12nm. Looking at Figure 10 it would suggest the LDV systems used a cantilever with a larger tip radius making it less sensitive to high-frequency spatial texture.

The surface roughness contrast is less apparent in the unfiltered LDV data (figure 8) due to a low frequency measurement drift in the LDV measured surface profile which appear as lines running parallel to the fast scan direction (bottom left to top right) over the surface in figure 8. This drift is more obvious in cross sections in the slow scan direction than the fast-scan (figure 9) and can be corrected for using a number of post-processing methods such as median line flattening[39]. Figure 10 shows the surface after implementing this compensation by sampling right to left and compares it to the OPU measured profile.

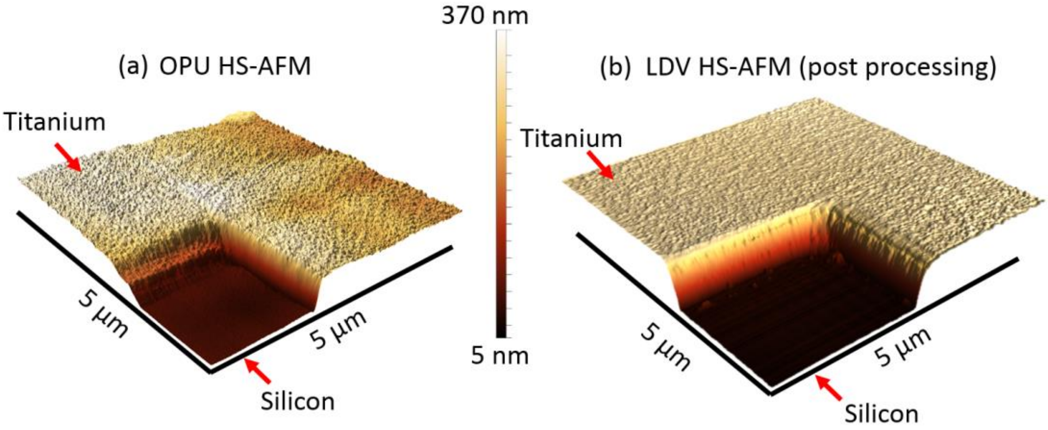

Figure 10: HS-AFM topography maps of titanium evaporated on silicon wafer as measured by two HS-AFM with different detection systems. The left shows the result of an OPU based system (a) and the right shows the results from a LDV based system (b) having used a median line removal.

We demonstrate the rapid scalability and stability of the OPU based instrument by extending our field of view beyond that of a single frame. By translating our high-speed window to 30 different, but overlapping (50 % overlap) locations, within 90 seconds, it is possible to generate a composite image. Figure 11, shows this composite image made of 3.65×10^6 uncompressed pixels. It is presented side-by-side with an equivalent LDV based HS-AFM composite image.

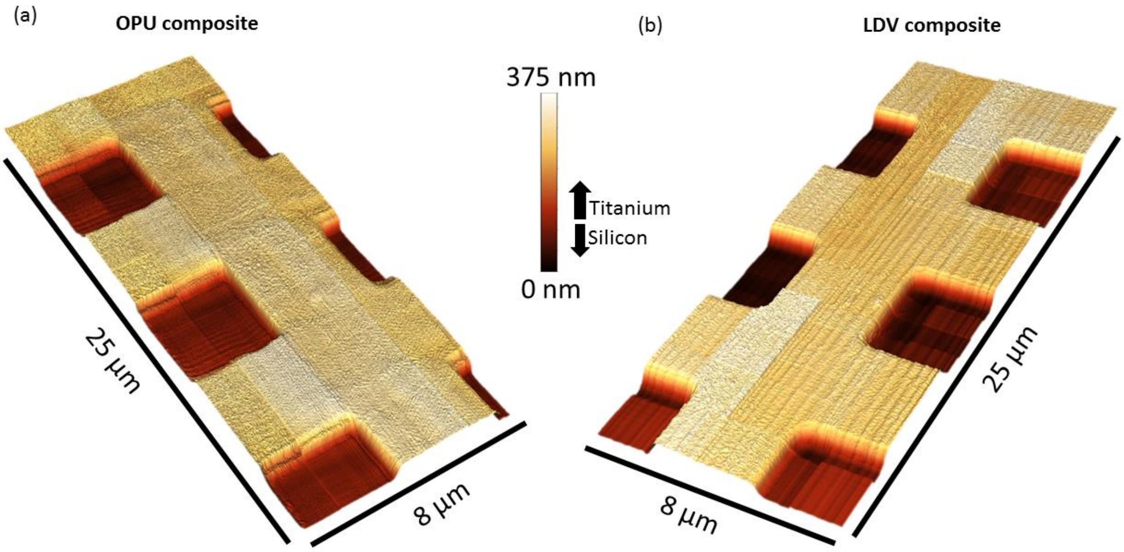

Figure 11. Composite images, from 30 sub frames without flattening, made by both the OPU (a) and LDV (b) based HS-AFMs. The composites are 3.65 megapixels in size and taken in less than 90 seconds with a mean tip velocity of 10 mm/s

Minor artefacts of stitching lines, cantilever oscillations and LDV drift can be seen in the resultant composite images as no post processing was done on the individual sub-frames used in creating the composite. These artefacts could be mitigated against via a number of post processing steps but would detract from the side by side comparison of unfiltered data generated by the two systems.

4. Discussion

The quality of these surface profiles demonstrates that an OPU detection system is a very suitable candidate for contact mode HS-AFM, capable of producing topographical surfaces equivalent to those obtained using a commercial HS-AFM. The consequence of such results gives promise of both the reduction in the cost of performing HS-AFM and a vast increase in measurement throughput (pixels per second). The authors have previously made use of this reported technique with Mikheykin et al. [29] in which two HS-AFMs, with either LDV or OPU detection system, carried out length assays of DNA molecules. In that work, the OPU-based HS-AFM was demonstrated to be capable of imaging DNA backbones of ~300 pm in height. Sub-nanometre resolution will likely be critical for other potential HS-AFM use cases such as the evaluation of atomic step heights in new classes of 2D materials [27].

Whilst the samples used for evaluation in this work focussed on 'hard' materials the OPU based instrument should be as equally versatile as other reports of this imaging mode. Previous works have shown the capability to image: in liquid[25], on soft materials [40] and of loosely adhered nanoscale bodies such as flakes of 2D materials or strands on genetic material (RNA/DNA) [27–29]. This technique is bounded by limitations common to most other forms of AFM e.g. not being able to image underneath overhanging features or objects unbound to a surface. Due to mechanical compliance-based feedback rather than active control, samples that require very fine control of surface load are less suitable for the OPU HS-AFM instrument. Future studies would look to evaluate the compatibility of the instrument with softer biological samples.

Key further work will look to take advantage of the low cost and mass-produced nature of the OPUs. Operating a set of these compact low-cost detection heads in parallel would enable multiple surface measurements to be made simultaneously, increasing the explored measurement area on a given sample per second. In addition, by utilising further bandwidth of the ADS (>45 MHz) the OPU detection head may be used to monitor higher modes (> 2nd) of the cantilever. Using the displacement measurements alongside the angular measurements offered by the ADS in frequency domain, further channels of information such as contact resonance or friction mapping can be explored [41].

5. Conclusion

In this work we have presented an OPU based HS-AFM and compared its performance with an equivalent LDV based HS-AFM. Results show that the resolution of the OPU based system can measure sub-nanometre, thermally excited, resonant modes of a commercially available AFM cantilever, agreeing with both a theoretical model and independent LDV measurements. Subsequently, the two instruments were used to perform HS-AFM over an area of 200 μm^2, generating 3.65 megapixel images in 90 seconds. In the presented HS-AFM images the OPU was shown to offer better unfiltered stability than the LDV. It is further postulated that, since the mechanical upper limit of this form of HS-AFM imaging has not yet been found, the imaging rate of the method can be increased to meet the maximum bandwidth of the detection OPU (which can exceed 100 MHz in some cases). We highlight how this research can be built upon in the formation of next generation high-speed AFMs. With the increasing demand for the characterisation of the building blocks within nanotechnology, we propose a route to utilising optical pickup technology to support this. The presented research has demonstrated OPUs as a scalable and sustainable toolset, due to it's low cost and relative simplicity, for exploring the nanoscale and extending these measurements up to macroscopic lengths.

Acknowledgements

We thank the EPSRC and the National Physical Laboratory for their financial support towards the research through the University of Bristol. Technical support and dedication from the University of Bristol mechanical and electronic workshop is gratefully acknowledged. Dr Picco and Dr Payton wish to thank the Royal Academy of Engineering for help with funding this research and NIST for providing the Si Ti sample.

Disclaimer

The naming of any manufacturer or supplier by University of Bristol, Bristol Nano Dynamics or The National Physical Laboratory in this scientific journal shall not be taken to be either University of Bristol’s Bristol Nano Dynamics or NPL’s endorsement of specific samples of products of the said manufacturer, or recommendation of the said supplier. Furthermore, University of Bristol, Bristol Nano Dynamics and NPL cannot be held responsible for the use of, or inability to use, any products mentioned herein that have been used by them.

References

1. Quercioli F, Tiribilli B, Bartoli a 1999. *Interferometry with optical pickups.* Opt Lett. **24** p:670–2.

2. Quercioli F, Tiribilli B, Ascoli C, Baschieri P, Frediani C 1999. *Monitoring of an atomic force microscope cantilever with a compact disk pickup*. Rev Sci Instrum. **70** p:3620–4.

3. Fan K-C, Chu C-L, Liao J-L, Mou J-I 2002. *Development of a high-precision straightness measuring system with DVD pick-up head*. Meas Sci Technol. **14** p:47–54.

4. Chu C-L, Chiu C-Y 2007. *Development of a low-cost nanoscale touch trigger probe based on two commercial DVD pick-up heads*. Meas Sci Technol. **18** p:1831–42.

5. Liao H-S, Huang K-Y, Hwang I-S, Chang T-J, Hsiao WW, Lin H-H, et al. 2013. *Operation of astigmatic-detection atomic force microscopy in liquid environments*. Rev Sci Instrum. **84** p:103709–7.

6. Liao H-S, Chen Y-H, Ding R-F, Huang H-F, Wang W-M, Hwu E-T, et al. 2014. *High-speed atomic force microscope based on an astigmatic detection system*. Rev Sci Instrum. **85** p:103710–7.

7. Bosco FG, Hwu E-T, Chen C-H, Keller S, Bache M, Jakobsen MH, et al. 2011. *High throughput label-free platform for statistical bio-molecular sensing.* Lab Chip. **11** p:2411–6.

8. Unger S, Ito S, Kohl D, Schitter G 2016. *Development of a compact atomic force microscope based on an optical pickup head*. IFAC-PapersOnLine. **49** p:629–35.

9. Hwu E-T, Hung S-K, Yang C-W, Hwang I-S, Huang K-Y 2007. *Simultaneous detection of translational and angular displacements of micromachined elements*. Appl Phys Lett. **91** p:221908.

10. Binnig G, Quate CF, Gerber CH 1986. *Atomic force microscope*. Phys Rev Lett. **56** p:930–3.

11. Meyer G, Amer NM 1988. *Novel optical approach to atomic force microscopy*. Appl Phys Lett. **53** p:1045–7.

12. Hansma PK, Cleveland JP, Radmacher M, Walters DA, Hillner PE, Bezanilla M, et al. 1994. *Tapping mode atomic force microscopy in liquids*. Appl Phys Lett. **64** p:1738–40.

13. Giessibl FJ 2000. *Atomic resolution on Si(111)-(7×7) by noncontact atomic force microscopy with a force sensor based on a quartz tuning fork*. Appl Phys Lett. **76** p:1470–2.

14. Picco L, Bozec L, Ulcinas A, Engledew DJ, Antognozzi M, Horton M, et al. 2007. *Breaking the speed limit with atomic force microscopy*. Nanotechnology. **18** p:044030–4.

15. Ando T 2013. *High-speed atomic force microscopy*. Microscopy. **62** p:81–93.

16. Payton OD, Picco L, Scott TB 2016. *High-speed atomic force microscopy for materials science*. Int Mater Rev. **61** p:473–94.

17. Payton OD, Picco L, Champneys AR, Homer ME, Miles MJ, Raman A 2011. *Experimental observation of contact mode cantilever dynamics with nanosecond resolution*. Rev Sci Instrum. **82** p:043704–5.

18. Payton OD, Picco L, Robert D, Raman A, Homer ME, Champneys AR, et al. 2012. *High-speed atomic force microscopy in slow motion—understanding cantilever behaviour at high scan velocities*. Nanotechnology. **23** p:205704–6.

19. Schitter G, Allgöwer F, Stemmer a 2004. *A new control strategy for high-speed atomic force miciroscopy*. Nanotechnology. **15** p:108–14.

20. Ando T 2008. *Control techniques in high-speed atomic force microscopy*. Proc Am Control Conf. p:3194–200.

21. Fantner GE, Schitter G, Kindt JH, Ivanov T, Ivanova K, Patel R, et al. 2006. *Components for high speed atomic force microscopy*. Ultramicroscopy. **106** p:881–7.

22. Bozchalooi IS, Youcef-Toumi K, Burns DJ, Fantner GE 2011. *Compensator design for improved counterbalancing in high speed atomic force microscopy*. Rev Sci Instrum. **82** p:1–12.

23. Ando T, Uchihashi T, Fukuma T 2008. *High-speed atomic force microscopy for nano-visualization of dynamic biomolecular processes*. Prog Surf Sci. **83** p:337–437.

24. Ando T, Uchihashi T, Kodera N, Yamamoto D, Taniguchi M, Miyagi A, et al. 2007. *High-speed atomic force microscopy for observing dynamic biomolecular processes*. J Mol Recognit. **20** p:448–58.

25. Pyne A, Marks W, Picco L, Dunton P, Ulcinas A, Barbour M, et al. 2009. *High-speed atomic force microscopy of dental enamel dissolution in citric acid*. Arch Histol Cytol. **72** p:209–15.

26. Casuso I, Rico F, Scheuring S 2011. *High-speed atomic force microscopy: Structure and dynamics of single proteins*. Curr Opin Chem Biol. **15** p:704–9.

27. Cullen PL, Cox KM, Subhan MK Bin, Picco L, Payton OD, Buckley DJ, et al. 2016. *Ionic solutions of two-dimensional materials*. Nat Chem. **9** p:244–9.

28. Miller TS, Suter TM, Telford AM, Picco L, Payton OD, Russell-Pavier F, et al. 2017. *Single crystal, luminescent carbon nitride nanosheets formed by spontaneous dissolution*. Nano Lett. p:acs.nanolett.7b01353.

29. Mikheikin A, Olsen A, Leslie K, Russell-Pavier F, Yacoot A, Picco L, et al. 2017. *DNA nanomapping using CRISPR-Cas9 as a programmable nanoparticle*. Nat Commun. **8** p:1665.

30. Shih H, Lu W, Chang J 2009. *Design of single-path optical pickup head with three wavelengths using integrated optical unit*. IEEE Trans Magn. **45** p:2202–5.

31. Bosco FG, Chen CH, Hwu ET, Bache M, Keller S, Boisen A 2011. *High-throughput automated system for statistical biosensing employing microcantilever arrays*. 2011 IEEE 24th Int Conf Micro Electro Mech Syst. p:877–80.

32. Morais S, Tamarit-López J, Carrascosa J, Puchades R, Maquieira A 2008. *Analytical prospect of compact disk technology in immunosensing.* Anal Bioanal Chem. **391** p:2837–44.

33. Donolato M, Antunes P, Zardán Gómez de la Torre T, Hwu E-T, Chen C-H, Burger R, et al. 2015. *Quantification of rolling circle amplified DNA using magnetic nanobeads and a Blu-ray optical pick-up unit*. Biosens Bioelectron. **67** p:649–55.

34. Hwu E-T, Liao H-S, Bosco FG, Chen C-H, Keller SS, Boisen A, et al. 2012. *An Astigmatic Detection System for Polymeric Cantilever-Based Sensors*. J Sensors. **2012** p:1–7.

35. Liao H-S, Chen Y-H, Ding R-F, Huang H-F, Wang W-M, Hwu E-T, et al. 2014. *High-speed atomic force microscope based on an astigmatic detection system*. Cit Rev Sci Instruments Rev Sci INSTRUMENTS. **85** .

36. Ulčinas A, Vaitekonis S 2017. *Rotational scanning atomic force microscopy*. Nanotechnology. **28** .

37. Hwu E-T, Huang K-Y, Hung S-K, Hwang I-S 2006. *Measurement of cantilever displacement using a compact disk/digital versatile disk pickup head*. Jpn J Appl Phys. **45** p:2368–71.

38. Stark RW, Drobek T, Heckl WM 2001. *Thermomechanical noise of a free v-shaped cantilever for atomic-force microscopy.* Ultramicroscopy. **86** p:207–15.

39. Klapetek P, Nečas D, Anderson C 2004. *Gwyddion user guide*. http://gwyddion.net/download/user-guide/gwyddion-user-guide-en.pdf.

40. Hobbs JK, Vasilev C, Humphris ADL 2005. *Real time observation of crystallization in polyethylene oxide with video rate atomic force microscopy*. Polymer (Guildf). **46** p:10226–36.

41. Shatil NR, Homer ME, Picco L, Martin PG, Payton OD 2017. *A calibration method for the higher modes of a micro-mechanical cantilever*. Appl Phys Lett. **110** p:223101.